Femtosecond multi-beam interference lithography based on dynamic wavefront engineering

Qiang Zhou,[1,2] Wenzheng Yang,[1] Fengtao He,[2] Razvan Stoian,[3] Rongqing Hui,[4] and Guanghua Cheng[1,3*]

[1]*State Key Laboratory of Transient Optics and Photonics, Xi'an Institute of Optics and Precision Mechanics, CAS, Xi'an 710119, Shaanxi China*

[2]*School of Electron and Engineering, Xi'an University of Post & Telecommunications, Xi'an 710121, Shaanxi China*

[3]*Laboratoire Hubert Curien, UMR 5516 CNRS, Université de Lyon, Université Jean Monnet, 42000 Saint Etienne, France*

[4]*Department of Electrical Engineering and Computer Science, University of Kansas, Lawrence, Kansas 66044, USA*

**gcheng@opt.ac.cn*

Abstract: A method for precise multi-spot parallel ultrafast laser material structuring is presented based on multi-beam interference generated by dynamic spatial phase engineering. A Spatial Light Modulator (SLM) and digitally programming of phase masks are used to accomplish the function of a multi-facet pyramid lens, so that the laser beam can be spatially modulated to create beam multiplexing and desired two-dimensional (2D) multi-beam interference patterns. Various periodic microstructures on metallic alloy surfaces are fabricated with this technique. A method of preparing extended scale periodic microstructures by loading dynamic time-varying phases is also demonstrated. Scanning electron microscopy (SEM) reveals the period and morphology of the microstructures created using this technique. The asymmetry of interference modes generated from the beams with asymmetric wave vector distributions is equally explored. The flexibility of programming the period of the microstructures is demonstrated.

OCIS codes: (070.6120) Spatial light modulators; (260.3160) Interference; (140.3390) Laser materials processing; (220.4000) Microstructure fabrication.

References and links

1. A. Lasagni, F. Mücklich, M. R. Nejati, and R. Clasen, "Periodical surface structuring of metals by laser interference metallurgy as a new fabrication method of textured solar selective absorbers," Adv. Eng. Mater. **8**(6), 580–584 (2006).
2. S. H. Kim, I. B. Sohn, and S. Jeong, "Parallel ripple formation during femtosecond laser grooving of ceramic," Appl. Phys., A Mater. Sci. Process. **103**(4), 1053–1057 (2011).
3. J. Serbin, A. Egbert, A. Ostendorf, B. N. Chichkov, R. Houbertz, G. Domann, J. Schulz, C. Cronauer, L. Fröhlich, and M. Popall, "Femtosecond laser-induced two-photon polymerization of inorganic-organic hybrid materials for applications in photonics," Opt. Lett. **28**(5), 301–303 (2003).
4. Y. H. Han and S. L. Qu, "Controllable fabrication of periodic hexagon lattice on glass by interference of three replicas split from single femtosecond laser pulse," Laser Phys. **19**(5), 1067–1071 (2009).
5. J. de Boor, N. Geyer, U. Gösele, and V. Schmidt, "Three-beam interference lithography: upgrading a Lloyd's interferometer for single-exposure hexagonal patterning," Opt. Lett. **34**(12), 1783–1785 (2009).
6. K. Kawamura, T. Ogawa, N. Sarukura, M. Hirano, and H. Hosono, "Fabrication of surface relief gratings on transparent dielectric materials by two-beam holographic method using infrared femtosecond laser pulses," Appl. Phys. B **71**(1), 119–121 (2000).
7. S. Yang, J. Ford, C. Ruengruglikit, Q. Huang, and J. Aizenberg, "Synthesis of photoacid crosslinkable hydrogels for the fabrication of soft biomimetic microlens arrays," J. Mater. Chem. **15**(39), 4200–4202 (2005).
8. J. H. Klein-Wiele and P. Simon, "Fabrication of periodic nanostructures by phase-controlled multiple-beam interference," Appl. Phys. Lett. **83**(23), 4707–4709 (2003).
9. M. Campbell, D. N. Sharp, M. T. Harrison, R. G. Denning, and A. J. Turberfield, "Fabrication of photonic crystals for the visible spectrum by holographic lithography," Nature **404**(6773), 53–56 (2000).

#183641 - $15.00 USD Received 16 Jan 2013; revised 29 Mar 2013; accepted 31 Mar 2013; published 12 Apr 2013

10. K. Kintaka, J. Nishii, A. Mizutani, H. Kikuta, and H. Nakano, "Antireflection microstructures fabricated upon fluorine-doped SiO2 films," Opt. Lett. **26**(21), 1642–1644 (2001).
11. X. Jia, T. Q. Jia, L. E. Ding, P. X. Xiong, L. Deng, Z. R. Sun, Z. G. Wang, J. R. Qiu, and Z. Z. Xu, "Complex periodic micro/nanostructures on 6H-SiC crystal induced by the interference of three femtosecond laser beams," Opt. Lett. **34**(6), 788–790 (2009).
12. H. Misawa, T. Kondo, S. Juodkazis, V. Mizeikis, and S. Matsuo, "Holographic lithography of periodic two- and three-dimensional microstructures in photoresist SU-8," Opt. Express **14**(17), 7943–7953 (2006).
13. J. Si, J. Qiu, J. Zhai, Y. Shen, and K. Hirao, "Photoinduced permanent gratings inside bulk azodye-doped polymers by the coherent field of a femtosecond laser," Appl. Phys. Lett. **80**(3), 359–361 (2002).
14. Y. Li, W. Watanabe, K. Yamada, T. Shinagawa, K. Itoh, J. Nishii, and Y. Jiang, "Holographic fabrication of multiple layers of grating inside soda–lime glass with femtosecond laser pulses," Appl. Phys. Lett. **80**(9), 1508–1510 (2002).
15. R. C. Gauthier and A. Ivanov, "Production of quasi-crystal template patterns using a dual beam multiple exposure technique," Opt. Express **12**(6), 990–1003 (2004).
16. N. D. Lai, J. H. Lin, Y. Y. Huang, and C. C. Hsu, "Fabrication of two- and three-dimensional quasi-periodic structures with 12-fold symmetry by interference technique," Opt. Express **14**(22), 10746–10752 (2006).
17. T. Kondo, S. Matsuo, S. Juodkazis, and H. Misawa, "Femtosecond laser interference technique with diffractive beam splitter for fabrication of three-dimensional photonic crystals," Appl. Phys. Lett. **79**(6), 725–727 (2001).
18. T. Kondo, S. Matsuo, S. Juodkazis, V. Mizeikis, and H. Misawa, "Multiphoton fabrication of periodic structures by multibeam interference of femtosecond pulses," Appl. Phys. Lett. **82**(17), 2758–2760 (2003).
19. Y. Hayasaki, M. Nishitani, H. Takahashi, H. Yamamoto, A. Takita, D. Suzuki, and S. Hasegawa, "Experimental investigation of the closest parallel pulses in holographic femtosecond laser processing," Appl. Phys., A Mater. Sci. Process. **107**(2), 357–362 (2012).
20. S. Hasegawa, Y. Hayasaki, and N. Nishida, "Holographic femtosecond laser processing with multiplexed phase Fresnel lenses," Opt. Lett. **31**(11), 1705–1707 (2006).
21. P. S. Salter and M. J. Booth, "Addressable microlens array for parallel laser microfabrication," Opt. Lett. **36**(12), 2302–2304 (2011).
22. M. Lei, B. L. Yao, and R. A. Rupp, "Structuring by multi-beam interference using symmetric pyramids," Opt. Express **14**(12), 5803–5811 (2006).
23. N. J. Jenness, K. D. Wulff, M. S. Johannes, M. J. Padgett, D. G. Cole, and R. L. Clark, "Three-dimensional parallel holographic micropatterning using a spatial light modulator," Opt. Express **16**(20), 15942–15948 (2008).
24. M. J. Escuti and G. P. Crawford, "Holographic photonic crystals," Opt. Eng. **43**(9), 1973–1987 (2004).
25. Z. Kuang, W. Perrie, J. Leach, M. Sharp, S. P. Edwardson, M. Padgett, G. Dearden, and K. G. Watkins, "High throughput diffractive multi-beam femtosecond laser processing using a spatial light modulator," Appl. Surf. Sci. **255**(5), 2284–2289 (2008).

1. Introduction

Femtosecond laser fabrication is an exciting and potentially practical technology for accurate processing of materials. Its major advantage derives from low thermal effects affecting the interaction region and subsequent high precision. In addition, the technique can be efficiently used on a large variety of materials (including metals, ceramics and polymers) due to a strong confinement of energy and nonlinear localized ablation [1–3]. However, the application of femtosecond laser fabrication is subject to various restrictions due to its low processing efficiency, triggering a strong effort into defining parallel processing technologies. The femtosecond laser interference lithography has the capability of single-step generation of precise microstructure patterns in large dimensions, which offers a parallel processing method of proven high efficiency [4]. Several other advantages can be stated such as no specific requirements for photomasks, and the possibility of breaking the diffraction limit of light so that nano-scale structures can be created [5]. The one dimensional (1D) fringe structure generated by two-beam interference has been widely used in grating fabrication [6]. In comparison, two dimensional (2D) and three dimensional (3D) light patterns which can be generated from multi-beam interference arrangements have promising applications in a large variety of photonic devices fabrication on surfaces and in the bulk. Examples include micro-lenses arrays [7], surface relief nanostructure [8], photonic crystals (PC) [9], functional surfaces [10, 11], and micro electro-mechanical systems (MEMS) [12].

The generation of precise interference patterns is rather challenging in various kinds of applications. A system of multi-beam interference is usually constructed with amplitude division mirrors, and optical delay stages in order to achieve certain spatial and temporal overlapping of the divided pulses [13, 14]. In fact, the major challenge of creating multi-beam

#183641 - $15.00 USD Received 16 Jan 2013; revised 29 Mar 2013; accepted 31 Mar 2013; published 12 Apr 2013

interference is the achieving of temporal superposition of the multiplexed femtosecond pulses. Controlling the temporal overlapping is typically based on nonlinear frequency conversion methods such as second harmonic generation (SHG) or third harmonic generation (THG). The levels of difficulty and complexity will enhance exponentially with the increase of the number of beams. Thus, there are no efficient ways to form 7 or more beams interference, and the fabrication of the complex quasi-periodic structure is limited to multiple and sequential exposure technology [15, 16].

There is an alternative method to form stable multi-beam interference, where the splitting system mainly consists of a diffraction beam splitter (DBS) and a confocal imaging system without the need of an optical delay stage [17, 18]. This technique is particularly useful for creating multi-beam interference of femtosecond pulsed beams since the temporal overlap of femtosecond pulses can be easily achieved with DBS. However, an aperture array, which was needed to select beams to form the desired interference pattern, usually leads to severe energy loss. Therefore it is very difficult to fabricate periodic structures on materials with a high ablation threshold which require strong optical power concentrations. Diffraction gratings can act as a phase mask, and interference can be formed by the first order diffraction beams [8], but its practicality is limited by the low diffraction efficiency, high cost and the lack of flexibility of gratings. Holograms based on Liquid-crystal Spatial Light Modulator (SLM) have the advantages of high-throughput pulsed irradiation and high energy efficiency. However, in practice it is very difficult to obtain uniform light spots even with the help of complex optimization algorithms [19–21].

A standard pyramid lens can form multi-beam interference easily with the benefits of low cost, high damage threshold and high transmission [22], and the spatial and temporal overlap of femtosecond pulses can also be guaranteed by the symmetry of the pyramid. However, each pyramid can only form one specific interference pattern because of the interference angle is confined by the base angle of the pyramid. Thus, the flexibility of using pyramid lenses is limited.

In this paper, a simple and flexible method to form multi-beam interference patterns based on a phase only SLM is presented. Multiple facet pyramids phases calculated according to actual pyramid lens technique were applied on the SLM to split a laser beam into several components of equal intensity and to form multi-beam interference. The method is useful for creating close packed periodic focal arrays, which is difficult using techniques such as holography. Moreover, in comparison with the DBS and the glass pyramid, the technique allows more easiness to control the structure and the period of the interference pattern by adjusting the facet number and base angle of the pyramid. Consequently, even various complex patterns formed by the interference of a large number of beams can be generated. To allow for sufficient energy density, the interfering pattern can be spatially demagnified and transferred onto the sample through a $4f$ imaging system and a focusing objective. The fabrication of periodic microstructures on metallic alloys surfaces is demonstrated, where scanning electron microscopy (SEM) images reveal a precise morphology of the microstructures. An efficient method of preparing large scale periodic microstructures is proposed, requiring simply loading dynamic phase patterns that achieve exposure without involving sample translation. Possible applications of this technique in anti-reflective surface microstructures for solar cells are indicated. The asymmetric interference mode generated from asymmetric phase masks is also explored for enhanced flexibility.

2. Method

Refraction at the surfaces of a wedge prism will introduce light deflection by a fixed angle θ, which is approximately given by

$$\theta \approx (n-1)\alpha, \tag{1}$$

#183641 - $15.00 USD Received 16 Jan 2013; revised 29 Mar 2013; accepted 31 Mar 2013; published 12 Apr 2013

where n is the refractive index of the prism material, and α is the base angle of the prism (defined as the angle between the prism base and its side facet). A prism that has an inclined phase front can manipulate a point in the image plane with a lateral displacement proportional to the base angle of the prism [23]. In a practical laser writing system, the lateral offsets between the laser focus and optical axis caused by a prism can be calculated by

$$\delta = f\theta, \tag{2}$$

with δ being the lateral shift of the laser focus, f being the focal length of the writing objective and θ being the deflection angle defined by Eq. (1). By changing the prism angle α, the location of the focus point in the focal plane can be precisely manipulated. This can be realized in a programmable way in SLM-based systems, where dynamic, varying spatial phase distributions of the laser beam can be modulated by controlling the refractive index distribution of the liquid crystal matrix. Rotating a prism and changing the prism angle at same time, one can steer the laser beam in the same way as a two dimensional galvanometer or a piezoelectric scanner. To realize the full potential of this method, we introduce a dynamic phase of the prism with a continuous variation of its base angle, followed by the rotation of the inclined phase. A helix structure was fabricated on the metallic alloy (0Cr18Ni9) surface without any mechanical movement, as shown in the Fig. 1. The change rate of the tilt angle and the rotation speed of the inclined phase codetermine the period of the helix.

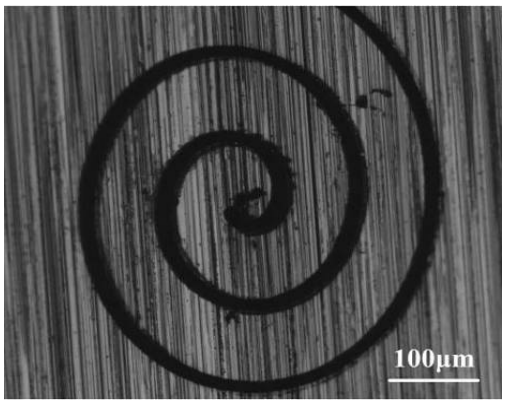

Fig. 1. Microscope image of the helix structure fabricated by dynamically inclined and rotating phase via a SLM. The laser writing power is 8 mW, rotation speed is 3°/s, and the focal length of focusing lens is 50 mm. Prism angle changes 0.2° per round.

Light beams passing through a symmetric multi-facet pyramid lens is comparable to the situation of one prism while multiplying the result in several directions, making this a straightforward solution for multiple output beams. Each part of the beam incident on a facet will have a different deflection direction and they could be coherently combined to form interference after the pyramid lens. The theoretical frame of using symmetric pyramid lens to form multi-beam interference and generate multiple light spots was elaborated in [22]. Briefly, the laser pulse, when transmitted along the optical axis of the pyramid lens, was divided into components of equal intensity which is determined by the number of the pyramid facets. The wave vectors of the divided beams distribute symmetrically along the optical axis. Thanks to the symmetry of the pyramid lens, the divided components would intersect to form interference in a domain defined by the initial beam size and the deflection angle and their temporal overlap is automatically achieved.

The interaction with the pyramid lens will impose a phase mutation on the light beam which is decided by the quantity: $\varphi(r) = (2\pi/\lambda)\Delta(r)$, where λ is the wavelength of the laser and $\Delta(r)$ is the optical path difference (OPD), determined by the pyramid lens' refractive index

#183641 - $15.00 USD Received 16 Jan 2013; revised 29 Mar 2013; accepted 31 Mar 2013; published 12 Apr 2013

n, and the base angle α. Via its programmable phase the SLM can efficiently work as a pyramid lens with variable refractive index and base angle to form multi-beam interference in a simple, straightforward and flexible method. We will verify the feasibility of this approach in the following sections.

First, we present the geometrical configuration of the phase masks corresponding to several multi-facet pyramid lenses, as shown in Figs. 2(a)-2(d). The 2D intensity distributions of the multi-beam interference patterns which are formed by multi-facet symmetric pyramid lenses with the parameters of $n = 1.5$ and $\alpha = 2°$ and variable number of facets were simulated with the MATLAB software and the plane wave approximation was employed in the calculation. The simulation is carried out to predict the potential irradiation results. For illustration purpose we only present the results of 3-beam, 4-beam, 25-beam and 50-beam interference patterns, as shown in Figs. 2(e)-2(h), other numerical examples can be found in [22].

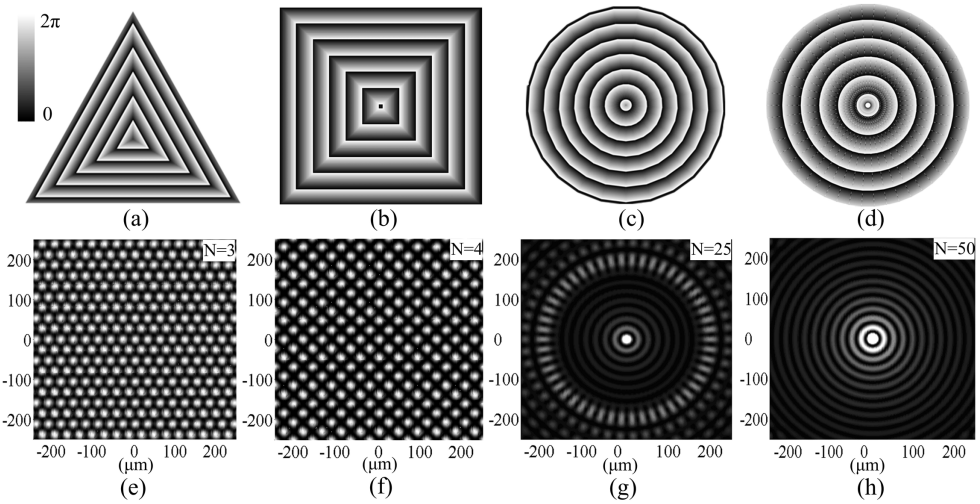

Fig. 2. Geometrical representation of the phase masks of several multi-facet pyramid lenses and the calculated intensity distribution of the interference patterns formed by multi-facet pyramid beam splitting. Phase masks of the (a) 3, (b) 4, (c) 25 and (d) 50 facets symmetric pyramid lenses (top) and the respective 2D intensity distributions of the interference patterns (bottom) for (e) 3, (f) 4, (g) 25 and (h) 50 facets symmetric pyramid lenses. The calculation parameters of the multi-facet pyramid lens are $n = 1.5$ and base angle $\alpha = 2°$. All the laser beams have the same original phase fronts and the wavelength of the laser radiation is 800nm. The interference pattern formed by a high number facet pyramid phase evolves gradually into a Bessel beam.

3. Experiment and results

3.1 Experimental setup for femtosecond laser interference

The experimental setup of the multi-beam interference system based on SLM phase modulation is schematically depicted in Fig. 3. Femtosecond laser pulses (with a 120 fs pulse duration, 800 nm center wavelength and 1 kHz repetition rate) are produced by a Ti:sapphire regenerative amplified laser system (Spitfire, Spectra Physics). The pulses were expanded and reflected on the calibrated SLM (HOLOEYE PLUTO phase modulator). The phase mask loaded on the SLM was calculated to simulate an actual multi-facet pyramid lens but with adjustable parameters. Considering the dynamic range of the SLM, all phases are given modulo 2π. The multi-beam interference with different characteristics can be formed by changing the phase mask, with a negligible influence of the 0 order. The generated light spots can be imaged by a charge-coupled device (CCD) equipped with a 10 × objective. For the purpose of periodic micro-structure fabrication, a $4f$ system and 10 × objective was used to transfer the interference

#183641 - $15.00 USD Received 16 Jan 2013; revised 29 Mar 2013; accepted 31 Mar 2013; published 12 Apr 2013

pattern to the sample surface. A dichroic mirror and CCD can monitor the pattern on sample surface in real-time.

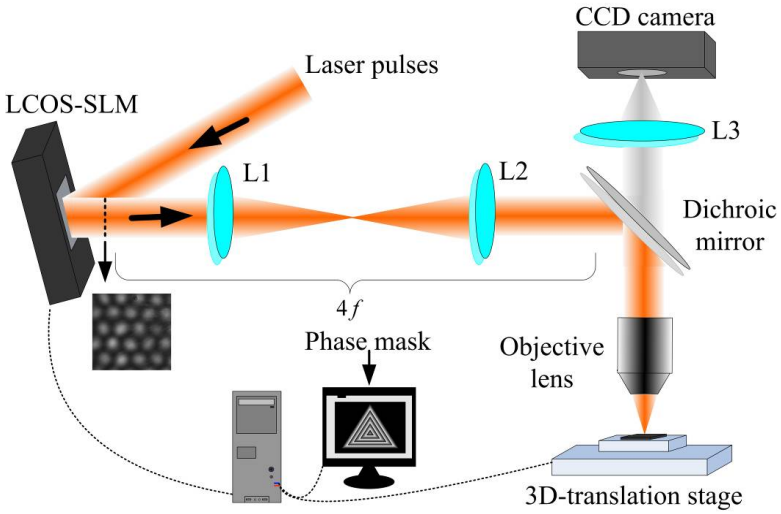

Fig. 3. Experimental setup for the multi-beam interference system. L1 and L2 are imaging lenses (f = 200 mm) in a 4f configuration. An objective lens was used to focus the formed spots onto the sample surface and via the dichroic mirror the CCD camera can monitor the sample surface in real-time. Different interference patterns were formed by changing the calculated phase masks.

3.2 Interference pattern formed by SLM

By loading the multi-facet pyramids phases, the multi-beam interferences were formed by SLM. The optical images of the phase-engineered 2D patterns which were generated from multi-beam interferences were captured by the CCD equipped with a 10 × objective, as shown in Fig. 4. The phase masks used in the experiment were calculated according to the practical pyramid lenses with the base angle of 2° and the refractive index of 1.5, similar to that used in the simulation previously discussed. Figures 4(a)-4(i) show the results of 3-beam, 4-beam, 5-beam, 7-beam, 9-beam, 15-beam, 25-beam, 40-beam and 50-beam interference patterns, respectively.

As can be observed, the intensity distributions of the three-beam interference pattern shown in Fig. 4(a) and four-beam interference pattern shown in Fig. 4(b) have the geometrical configurations of hexagon and square, respectively. The measured period of the symmetrical hexagon lattice shown in Fig. 4(a) and square lattice shown in the Fig. 4(b) are about 26 μm and 33 μm, respectively. They are in agreement with the theoretical value of 26.5 μm for three-beam interference and 32.4 μm for four-beam interference as calculated by [24]:

$$d_{3-beam} = (2/\sqrt{3}) \cdot \lambda / (2\sin\theta) = \lambda / (\sqrt{3}\sin\theta) \quad (3)$$

$$d_{4-beam} = \sqrt{2}\lambda / (2\sin\theta) = \lambda / (\sqrt{2}\sin\theta), \quad (4)$$

where λ is the wavelength of the laser and θ is the interference angle, which is approximately equal to half of the base angle of the pyramid lens when the base angle is small enough. In fact, using Eq. (1) based on the refraction theorem, if the refractive index of the pyramid lens is $n = 1.5$, we can find $\theta = \alpha/2$, where α is the base angle of the pyramid lens. Obviously, the period of the lattice will decrease with increasing base angle when the other laser parameters are invariable.

#183641 - $15.00 USD Received 16 Jan 2013; revised 29 Mar 2013; accepted 31 Mar 2013; published 12 Apr 2013

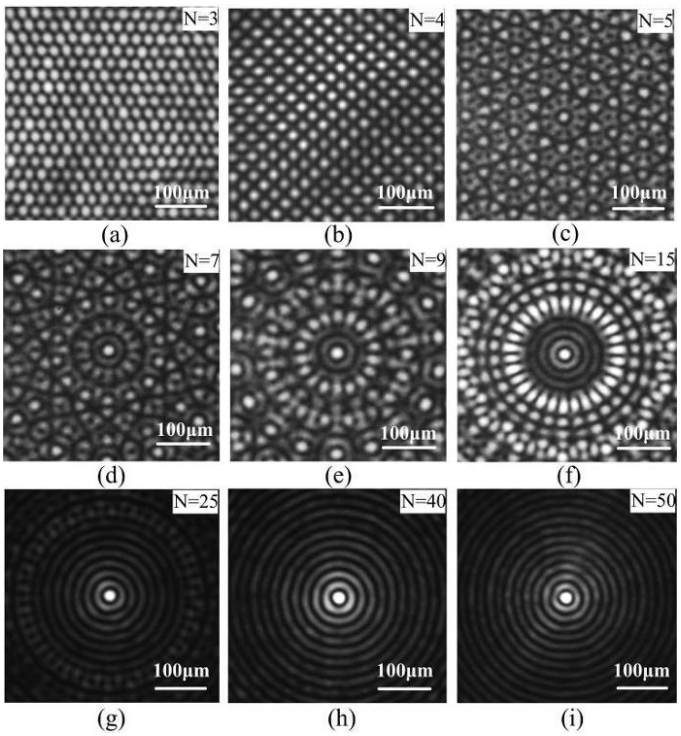

Fig. 4. Optical images of the results of experimental multi-beam interferences for (a) 3 beams, (b) 4 beams, (c) 5 beams, (d) 7 beams, (e) 9 beams, (f) 15 beams, (g) 25 beams, (h) 40 beams and (i) 50 beams. The phase masks used in the experiment are calculated according to actual symmetric pyramid lenses with the parameters of $n = 1.5$, and $\alpha = 2°$. The images were captured by a CCD equipped with a 10 × objective; the scale bar is 100 μm.

The first glimpse of the higher complexity pattern formed by an increasing number of interfering beams (5 beams, 7 beams, 9 beams, 15 beams and 25 beams interference) depicted in Figs. 4(c)-4(g) show an evolution away from the rectangular symmetry, although they still have periodic structures. The pattern formed by 5 beams interference shown in Fig. 4(c) has some resemblance to a quasi-crystal lattice, and the patterns formed by 9 beams, 15 beams and 25 beams interference have interesting lattice distributions of increasing circular symmetry. Enhancing the number of facets of the pyramid lens, the multi-facet pyramid lens will approach an axicon form. By loading the 40-facet and 50-facet pyramid lens phases into SLM, the 40-beam and 50-beam interference patterns are shown in Fig. 4(h) and Fig. 4(i), which come close to the pattern of a zero-order Bessel beam.

Comparing the experimental results shown in Fig. 4 with the simulated results shown in Fig. 2, the agreement between them is obvious in both the geometrical configurations and the periods within the patterns. The agreement between experimental and calculated intensity distributions extends also for various other parameters which are not shown here. This confirms that SLM with proper phase pattern design can be used to replace pyramid lenses with high accuracy and flexibility. We note that the limited bandwidth of the laser does not produce observable chromatic effects.

3.3 Periodic micro-structures fabrication by symmetric pyramid phases

A number of periodic structures were fabricated on metallic alloy (0Cr18Ni9) surfaces by using the multi-spot patterns generated from the interference technique described above. The phase masks used in the fabrication were calculated based on the 3-facet and 4-facet pyramid lens, with the base angle of 2°respectively, and both three-beam and four-beam interference patterns

#183641 - $15.00 USD Received 16 Jan 2013; revised 29 Mar 2013; accepted 31 Mar 2013; published 12 Apr 2013

were formed to fabricate periodic structures. The axial extension of the interference region encompassing the presence of multiple interfering light spots with a constancy in the resulting pattern (which can be calculated as $Z \approx \omega / \tan\theta$, where $\omega = 4.32$ mm is the radius of the laser spot and $\theta = 1°$ is the interference angle) was about 25 cm, starting at the SLM position. For the convenience of the experiment, a $4f$ system (f = 200 mm) was used to transfer the multiple light spots pattern further away from the SLM surface. A 10 × objective lens (NA = 0.25) was employed to image the laser beam on the sample surface to achieve a high laser fluence and demagnify the period of the interference patterns. The objective was placed at 150 mm behind the last focal plane of the $4f$ system, so that the period of the interference patterns can be compressed by ten times. The extension of the depth of field is related to the initial interference domain and the demagnification factor of the imaging system, allowing equally a certain tolerance in positioning the objective. The real-time CCD monitoring of the sample surface via the dichroic mirror can inspect the pattern distribution on the sample. The morphology details of the fabricated structure were post mortem imaged using a high-resolution scanning electron microscope (SEM).

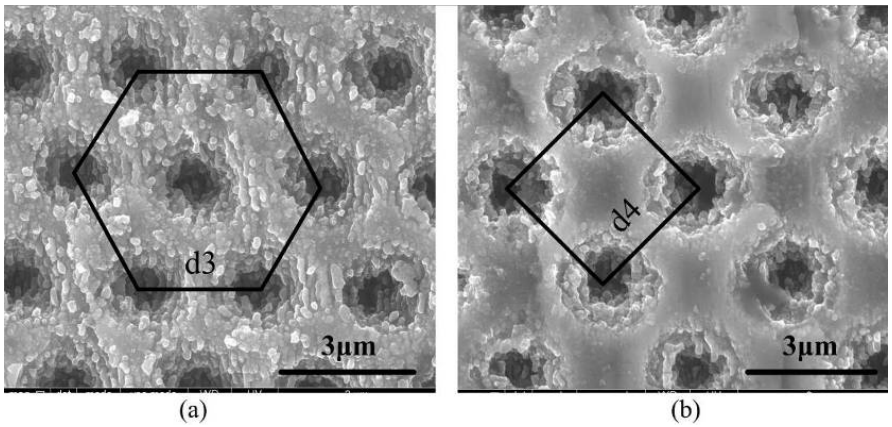

Fig. 5. SEM images of the structures fabricated by (a) three-beam and (b) four-beam interference of fs pulses, the used phase masks are calculated according to the 3-facet pyramid lens and 4-facet pyramid lens with the base angle of 2°. The power of the laser is 20 mW and the exposure time is 10 s.

Figure 5 demonstrates the SEM images of the structures fabricated by three-beam interference and four-beam interference. The fabricated patterns shown in Figs. 5(a) and 5(b) clearly reveal the lattice structures of hexagon and square, respectively, and the period of the hexagon structure is about 2.7 μm while the parameter of the square structure is about 3.4 μm. There is a good agreement with the calculated values of 2.6 μm and 3.3 μm assuming 10 × image demagnification ratios. The minor discrepancies may be caused by the tolerances in localizing the surface with respect to the image plane of the objective. Both the shape and the period of the fabricated structures are consistent with the anticipated character of the spots formed by multi-beam interference. This agreement confirms that the periodic structures were in fact fabricated by the interference of the laser beams directly.

3.4 Dynamic phase for large scale microstructure fabrication

To fabricate surface microstructures on a large scale, the practical technique requires mechanically translating the sample with respect to the laser beam. However the processing efficiency is limited by the speed and accuracy of mechanical movement of the stage and, to some extent, also the achievable complexity degree. The SLM based optical system offers great flexibility in manipulating each individual light beam in a complex multi-beam arrangement. It

#183641 - $15.00 USD Received 16 Jan 2013; revised 29 Mar 2013; accepted 31 Mar 2013; published 12 Apr 2013

provides a straightforward way to fabricate large scale micro-structures of complex patterns, without the need of mechanically moving the sample [25].

It is well known that a single facet prism with an inclined phase can manipulate light spots with lateral displacements in the image plane. Also, this concept is not exclusive to a single point, and it can be applied to multi-spots [23]. By adding an inclined phase to the phase of four-facet pyramid, the multi-spot pattern formed by four-beam interference would generate a lateral displacement in the image plane, which can be calculated from Eq. (2), where δ should be the lateral shift of the entire pattern. The total phase may be calculated by

$$Phase_{total} = \mathrm{mod}(Phase_{pyramid} + Phase_{prism}, 2\pi). \quad (5)$$

Using this method, we scanned the complex pattern formed by four-beam interference via the displacements in the image plane and fabricated a large scale microstructure on GaAs substrate without mechanically actuating the sample. The description of the process and the corresponding phase masks are shown in Fig. 6(a). In the laser irradiation area, a 30 × 30 multi-spot pattern with the scale of about 100 μm × 100 μm was fabricated in parallel at first. In order to eliminate disturbances by heat or interference through the subsequent steps, the entire multi-spot area is then phase-shifted by 100 μm to complete the final structures. So the inclined phase is stepwise changed with each base angle value of the prism accountable by the Eqs. (1) and (2).

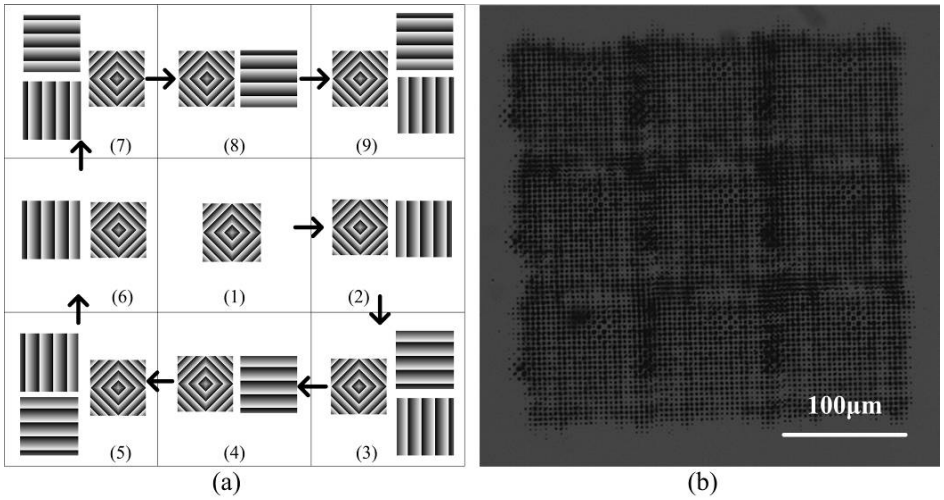

Fig. 6. Depiction of the process of the large scale microstructure fabrication by dynamic phase variations. (a) Phase shift patterns and (b) microscope image of the large scale concave structures fabricated by dynamic phase shift method. The power of the laser is 20 mW and the exposure time is 10 s.

By shifting the phase and controlling the exposure time by the shutter, an overall 90 × 90 pattern of concave structures with the scale of about 300 μm × 300 μm was fabricated without mechanical movement of the sample. The microscope image of the experimental demonstration is presented in Fig. 6(b). In the practical fabrication process the lateral displacement of the multi-spot may cause aberrations and lead to the defect of the structures. However, considering the resolution of the SLM and the low base angle value of the single facet prism, as well, the experimental imaging/focusing parameters (the focal length of the objective is 16 mm and the base angle of the single facet prism calculated by Eqs. (1) and (2) was $\alpha = 0.72°$), the aberrations caused by the single facet prism are small. We note however the presence of edge effects caused by the intensity distribution of the spots determined by the Gaussian apodization of the incident beam and the presumable influence of the field curvature in the imaging process.

#183641 - $15.00 USD Received 16 Jan 2013; revised 29 Mar 2013; accepted 31 Mar 2013; published 12 Apr 2013

It is conceivable that Fourier spatial filtering may improve the pattern quality, an aspect not investigated here.

3.5 Asymmetry interference mode generation

The multi-beam interference was not only limited to beams with symmetric waveform distribution. A more prevalent situation is where the wave vector of each beam is distributed asymmetrically along the propagation direction. The distribution of the wave vectors will decide the structural form of the interference pattern. The SLM can also easily form multi-beam interference patterns with the wave vectors of the beams asymmetrically distributed.

Two-beam interference formed by a symmetric double facet prism will generate a fringe structure, as shown in Fig. 7(a). This is a pattern widely used in grating fabrication. To be able to fabricate period-variable gratings, one of the facets of the prism can be replaced by a paraboloid. By loading this asymmetrical prism phase, an asymmetrical interference pattern with a varying period was obtained, as shown in Fig. 7(b). The controlling of the spatially varying period of the grating structure can be achieved by changing the curvature of the paraboloid.

As to three beam interference, we change one of the prism angles from 1°to 2°in a 3-facet pyramid lens phase and compare the resulting interference pattern with that of symmetric facets. As shown in Figs. 7(c) and 7(d), the pattern of the interference pattern changes from a regular hexagon to an increasingly irregular hexagonal form.

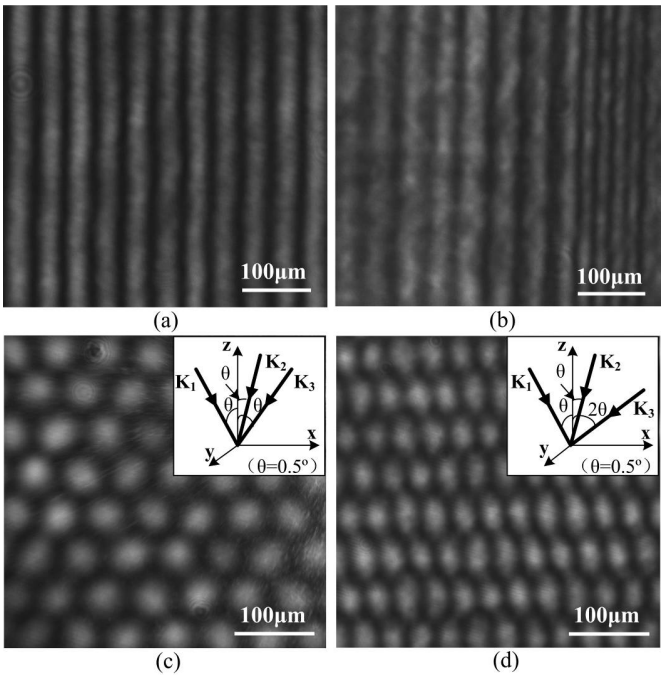

Fig. 7. Comparison of the symmetrical and asymmetrical interference modes and corresponding optical patterns. Two-beam interference pattern of (a) period-fixed grating structure formed by two beam symmetric interference and (b) period-variable grating structure formed by asymmetric interference with half prism half parabolic masks. Three-beam interference pattern for (c) regular hexagon structure formed by symmetric interference in three equivalent facet pyramid lens and (d) irregular hexagon structure formed by asymmetric interference. The inset depicts the distribution of the wave vectors.

#183641 - $15.00 USD Received 16 Jan 2013; revised 29 Mar 2013; accepted 31 Mar 2013; published 12 Apr 2013

4. Conclusion

In conclusion, we have demonstrated that a SLM with numerically created phase masks can be used as a multi-facet programmable pyramid lens to form complex and flexible multi-beam interference patterns. By loading different phase masks calculated according to the symmetrical pyramid lens with various parameters and facets number, we were able to obtain multi-spot patterns with different lattice structures and periodicities. We were also able to create complex quasi-periodic structures through interference between 7 or more light beams. The fabrication of periodic microstructures on solid materials by using multi-spot interference technique was demonstrated. Extended area microstructures were also fabricated with phase-only pattern shift. The impact of asymmetric phase distribution on pattern creation was investigated. The predicted characteristics are in good agreement with the experimental results. The optical system based on SLM is simple, yet powerful and practical, and has the potential to replace rather complicated optical systems including multiple diffractive and refractive elements.

Acknowledgments

The authors acknowledge the support given by the West Light Foundation of The Chinese Academy of Sciences, National Natural Science Foundation of China (No.61223007), and the French Agence Nationale de la Recherche.

#183641 - $15.00 USD Received 16 Jan 2013; revised 29 Mar 2013; accepted 31 Mar 2013; published 12 Apr 2013